

Soil depth as a driver of microbial and carbon dynamics in a planted forest (*Pinus radiata* D. Don.) pumice soil

Alexa K. Byers¹, Loretta G. Garrett², Charlotte Armstrong³, Fiona Dean², Steve A. Wakelin³

5 ¹Bioprotection Aotearoa, PO Box 85084, Lincoln University, Lincoln, 7674, New Zealand

²Scion, Private Bag 3020, Rotorua, 3046, New Zealand

³Scion, PO Box 29237, Riccarton, Christchurch, 8440, New Zealand

10 *Correspondence to:* Alexa K. Byers (alexa.byers@lincoln.ac.nz)

Abstract. Forest soils are fundamental in regulating the global carbon (C) cycle; their capacity to accumulate large stores of C means they form a vital role in mitigating the effects of climate change. Understanding the processes that regulate forest soil organic C (SOC) dynamics and stabilisation is important to maximise the capacity and longevity of C sequestration. Compared to surface soil layers, little is known about the SOC dynamics in subsoil layers, *sensu* those below 30 cm depth. This knowledge 15 gap creates large uncertainties when estimating the distribution of global soil C stocks and assessing the vulnerability of SOC reserves to climate change. This study aimed to dive deep into the subsoils of Puruki Experimental Forest (New Zealand) and characterise the changes in SOC dynamics and the soil microbiome down to 1 metre soil depth. ITS and 16S rRNA sequencing and quantitative real-time PCR were used to measure changes in soil microbial diversity, composition and abundance. Stable ($\delta^{13}\text{C}$) and radioactive (^{14}C) C analyses were performed to assess depth driven changes in SOC stability and age. Our research 20 identified large declines in microbial diversity and abundance with soil depth, alongside significant structural shifts in community membership. Importantly, we conservatively estimate more than 35% of total C stocks are present in subsoil layers below 30 cm. Although C age steadily increased with depth, reaching a mean radiocarbon age of 1571 yBP (years before present) in the deepest soil layers, the stability of SOC varied between different subsoil depth increments. These research 25 findings highlight the importance of quantifying subsoil C stocks for accurate C accounting. By performing a broad range of analytical measures, this research comprehensively characterised the abiotic and biotic properties of a subsoil environment - a frequently understudied but significant component of forest ecosystems.

1 Introduction

Forest soils are influential in regulating the global C cycle, accounting for over 70% of the world's soil organic C (SOC) reserves and supporting over 80% of the total aboveground terrestrial C stocks (Batjes, 1996; Jobbágy and Jackson, 2000; Six 30 et al., 2002). Developing forest management strategies which maximise soil C sequestration will, therefore, serve as a powerful tool for offsetting fossil fuel emissions and mitigating against climate change (Jandl et al., 2007; Mukul et al., 2020).

Compared with surface soil layers, the deeper subsoil layers of forest ecosystems are comparatively underexplored (Yost and Hartemink, 2020). Although the concentration of soil organic C (SOC) declines with depth (Schmidt et al., 2011), studies have reported that, accumulatively, up to 50% of total SOC may be contained within soil layers below 30 cm (Balesdent et al., 2018; 35 Jobbágy and Jackson, 2000; Gonzalez et al., 2018; Ross et al., 2020).

Deep SOC is more resistant to decomposition by soil microorganisms due to the biological, physical, and chemical conditions of the subsoil environment (Schmidt et al., 2011). Thus, when undisturbed, deep SOC is considered to represent the ‘stable’ fraction of the SOC pool. However, the stability of sequestered SOC is complex and is related to a range of variables including soil clay content, mineralogy, structure and texture, landscape position, association with microaggregates, climate, and 40 vegetation (Jobbágy and Jackson, 2000; Lal, 2004). Furthermore, stability of SOC is strongly influenced by the activities of plant roots, and soil microorganisms (Kuzyakov, 2010; Song et al., 2020). The historical biases against sampling deeper soil layers means we have a limited understanding on how the properties of subsoil environments influence their ability to sequester and store SOC. This introduces uncertainty when modelling the stability of deep SOC pools to climate change (Gross and Harrison, 2019).

45 Soil microorganisms are responsible for the transformation and stabilisation of SOC (Lladó et al., 2017; Spohn et al., 2016) and are influential in determining patterns of C sequestration (Jastrow et al., 2007). Studying the changes that occur to soil microbial communities with depth is essential to understand the extent and nature of their role in regulating long-term SOC dynamics. Previous studies have reported that soil microbial diversity, abundance, respiration, and C turnover declines with depth (Blume et al., 2002; Eilers et al., 2012; Fang et al., 2005; Fierer et al., 2003; Spohn et al., 2016). More recent research 50 has explored the taxonomic and functional changes that occur in microbial communities with soil depth (Brewer et al., 2019; Frey et al., 2021; Hao et al., 2021). However, particularly for coniferous forest ecosystems, our knowledge on the response of soil microbial communities to depth and the environmental properties driving these changes remains poorly understood. Furthermore, the inherently heterogeneous nature of soil environments, both globally and locally (Curd et al., 2018; Kuzyakov and Blagodatskaya, 2015; Štursová et al., 2016), means context-specific research is required to understand the SOC dynamics 55 and associated microbiota of forest subsoil environments. To maximise the sink capacity of forest soils and to retain the SOC already stored at depth, we need to better understand the processes that regulate C sequestration and long-term C storage within the deep soil environment.

Using Puruki Experimental Forest (central North Island, New Zealand) as a case study, this research aimed to improve our understanding of subsoil C dynamics within a production forest. Using a wide range of analytical methods, we aimed to 60 examine the variability in subsoil C dynamics in 10 cm increments down a 1 metre soil profile. Changes in the diversity, composition, and abundance of bacterial and fungal communities with depth were quantified using 16S/ITS rRNA amplicon sequencing and quantitative real-time PCR (qPCR). Measurements of natural ^{13}C abundances in soils has previously been used to study SOC dynamics, with the isotopic composition ($^{13}\text{C}/^{12}\text{C}$ ratio) of soils functioning as a proxy for soil C turnover (Garten et al., 2008; Paul et al., 2020; Poage and Feng, 2004; Wang et al., 2018). Therefore, to better understand changes in C cycling 65 dynamics down each soil core, the isotopic composition of each depth increment was measured. Radiocarbon aging based off

measurements of ^{14}C abundance was further used to identify older stabilised C stocks (Chabbi et al., 2009). The results of this research contribute to our understanding of the biological and chemical properties of productive forest subsoil environments, a critical research gap that is fundamental for assessing the vulnerability of forest SOC stocks to climate change.

2 Materials and Methods

70 2.1 Study site and soil collection

Soils were sampled from Puruki Experimental Forest ($38^\circ 26'\text{S}$, $176^\circ 13'\text{E}$), located in the Paeroa Range of New Zealand's central North Island (Figure A1). Puruki Experimental Forest (henceforth referred to as Puruki Forest), is a 35-hectare *Pinus radiata* forest which was established in 1973, after previously being converted from podocarp/hardwood native forest to rye grass and clover pasture in 1957 (Beets and Brownlie, 1987; Garrett et al., 2021). Puruki Forest is now near the end of its 75 second rotation, having previously been harvested in 1997 (Oliver et al., 2004). Puruki Forest was selected for investigation due to its high scientific impact and extensive contribution to production forestry research (Garrett et al., 2021). Furthermore, Puruki Forest has an extensive body of historical data available related to soil health, productivity, and land management; factors which are all vitally important for helping us understand drivers of subsoil C dynamics (Garret et al., 2021).

Puruki Forest sits at an elevation range of 500 to 700m a.s.l., varies from gently (less than 12°) to steeply sloping (up to 30°) 80 land, with a mean annual rainfall of 1500 mm and mean annual temperature of 10°C (Beets and Brownlie, 1987; Brownlie and Kelliher, 1989). Puruki Forest has an average soil pH of 5.2 at 0 to 10 cm depth (Beets and Brownlie, 1987). The soil pH at Puruki Forest has been reported to increase with depth, having an average pH of 5.62 at 1 to 2 m depth (Beets et al., 2004). Soil parent materials originated from Taupo volcanic centre (1850 ± 100 BP) and older ash showers from Taupo and Okataina 85 volcanic centres (Rijkse and Bell, 1974). The area's Orthic Pumice soils are highly permeable, being composed of loamy sand, silty sand, and gravel (Taupo lapilli) (New Zealand Soil Classification System; Hewitt, 2010).

A permanent sample plot (PSP) within the Rua sub-catchment of Puruki Forest was targeted for sampling. As Puruki has a varied topology, our sampling plot was located along a 12° slope. Soils were collected just outside of the plot to avoid disturbance for longer term monitoring at the site. For sampling, 10 points spaced 2 metre (m) apart were set out along an 18 m transect. At each sampling point, two paired 1 m soil cores were extracted using a motorised percussion soil sampler capable 90 of collecting intact cores with an internal plastic sleeve; one core was taken for bulk density analysis and the other used for DNA and chemistry analysis. Following extraction, core pairs were visually compared to check for any considerable differences in soil colour and texture by depth (Figure A2). Intact soil cores were transported back to the lab in cool, dark conditions. Care was taken to minimise disruption during transport so that cores remained intact from field to lab. Following transport, soil cores were divided into 10 cm increment samples. Incidences of compaction which occurred during sample 95 collection were adjusted for during the division of cores into depth increments (Supplementary Methods).

2.2 Sample preparation

To prepare soils for DNA analysis, moist soil samples were sieved to less than 2 mm and stored at -20°C until ready for DNA extractions. DNA was extracted from 0.25 g of each soil sample using a DNeasy Powersoil Pro Kit (Qiagen) according to manufacturer's instructions. Soils required for measurements of total C & nitrogen (N), total phosphorus (P), Bray P, pH, 100 Mehlich 3 extractable elements (Ca, K, Mg, and Na), cation exchange capacity (CEC), exchangeable cations, organic P and inorganic P analysis were air dried and sieved to <2 mm. For measurements of bulk density, air dried fine (<2 mm) and coarse (>2 mm) soil fractions were oven dried separately at 104°C until a constant weight. Subsamples of air-dried soils were fine ground using a Spex800D ball mill for measurements of total C (%), total N (%), $\delta^{13}\text{C}$ [‰], and radiocarbon ^{14}C analysis [‰].

2.3 Soil chemistry

105 Total C and N were determined on fine (<2 mm) and coarse (>2 mm) fraction fine ground soils by dry combustion using a LECO CNS-2000 carbon nitrogen analyser (Rayment and Lyons, 2011). Soil pH was determined in water at a soil: water ratio of 1:2.5 (Blakemore et al., 1977). Total phosphorus (P) was measured by flow injection analyser (FIA) colorimetry after sulphuric acid digestion (Blakemore et al., 1977; Taylor, 2000). Bray P was measured by FIA colorimetry after sequential Bray 2 ($\text{NH}_4\text{F}/\text{HCl}$) extraction at a ratio of 1:10 soil: extractant (Blakemore et al., 1977; Bray and Kurtz, 1945). Exchangeable 110 cations (Ca, K, Mg, and Na) were measured by inductively coupled plasma mass spectrometry (ICP-MS) after 1:50 (macro) $\text{NH}_4\text{CH}_3\text{COO}$ leaching. Cation exchange capacity (CEC) was measured by FIA colorimetry after 1M NH_4COOH leaching, followed by 1M NaCl (Blakemore et al., 1977; Sparks et al., 1996).

2.3.1 Stable isotope ($\delta^{13}\text{C}$) analysis

115 Fine ground soil samples were sent to GNS Stable Isotope Laboratory (Wellington, New Zealand) for $\delta^{13}\text{C}$ analysis by isotope ratio mass spectrometry. Soil samples were pre-treated by adding 10% HCl to 1 g of each sample and left overnight at room temperature. Samples were then centrifuged and rinsed to neutral pH. Following pre-treatment, samples were freeze dried and measured on an Isoprime mass spectrometer using a Eurovector elemental analyser. All $\delta^{13}\text{C}$ results are reported with respect to VPDB and N-Air, normalized to GNS internal standards which were cane sugar (-10.3‰), beet sugar (-24.6‰), and EDTA (-31.1‰). The stable carbon isotope composition ($^{13}\text{C}/^{12}\text{C}$) is reported in $\delta^{13}\text{C}$ values presented as per thousand [per mille, ‰], 120 with the analytical precision for these measurements being 0.2‰.

2.3.2 Radiocarbon ^{14}C analysis

Fine ground soil samples were graphitized at the Houghton Carbon, Water and Soils Lab (USDA Forest Service Northern Research Station, Michigan, US) and radiocarbon measurements were conducted at the DirectAMS facility (Bothell, Washington, US). Soil samples were combusted at 900°C for 6 hours in evacuated, sealed quartz tubes with cupric oxide 125 (CuO) and silver (Ag) wire to form CO_2 gas. After combustion, CO_2 was reduced to graphite through heating at 570°C with

hydrogen (H_2) gas and an iron (Fe) catalyst (Vogel et al., 1987). Graphite targets were analysed for radiocarbon abundance using accelerator mass spectrometry (AMS) and corrected for mass dependent fractionation using measured $\delta^{13}C$ values according to Stuiver and Polach (1977). Conventional Radiocarbon Age (CRA) and ^{14}C are reported as defined by Stuiver and Polach (1977), with CRA presented as years before present (yBP) and ^{14}C presented as per thousand [per mille, ‰].

130 2.4 Microbial amplicon sequencing

Following the Earth Microbiome Project (EMP) protocols, barcoded forward and reverse primers 515F-806R were used to amplify the 16S rRNA V4 region (Caporaso et al., 2012). Nested PCRs were performed on DNA samples which initially failed to amplify using the non-barcoded primers 27F-1492R. Following nested PCR, amplicons were amplified using barcoded 515F-806R primers. The EMP's standard ITS amplicon protocol was followed to amplify the fungal ITS gene region using 135 the barcoded primers ITS1f-ITS2 (Bokulich and Mills, 2013; Hoggard et al., 2018). DNA samples which initially failed to amplify were targeted for nested PCR using primers NSA3-ITS4. Nested PCR products were PCR amplified using the barcoded primers ITS1f-ITS2. Full details of the PCR reaction protocols are provided in the Supplementary Materials. Successful PCR amplicons were sent for Illumina 500 MiSeq 250bp (16S rRNA) and Illumina 600 MiSeq 300 bp (ITS rRNA) paired-end sequencing at the Australian Genome Research Facility (AGRF; Melbourne, Australia). For the 16S rRNA 140 amplicon libraries, eight no-template control (NTC) samples, which showed no visible bands during agarose gel electrophoresis, were sent for sequencing to check for contaminants.

2.5 Quantitative PCR

The absolute concentration of bacterial and fungal DNA in each DNA sample was determined from standard curves using AriaMx SYBR Green qPCR (Agilent Technologies). Broad range forward and reverse primers 338F-518R and ITS1F-5.8s 145 were selected to target the 16S rRNA (V3-V4) and ITS gene region for quantification (Shahsavari et al., 2016). Full details of the qPCR reaction protocol and standard curve preparation are provided in the Supplementary Methods. Following quantification, 16S and ITS rRNA copy numbers were adjusted to copy number per ng DNA.

2.6 Statistical analysis

Prior to analysis, slope corrected C stocks ($Mg\ ha^{-1}$) were calculated based on total C (%) and soil bulk density measurements. 150 Slope corrected stocks were calculated using the following formula: '($BD \times SOC_{conc} \times D$) $\times SF$ ' (Gattinger et al., 2012; Jones et al., 2008). Where 'BD' is bulk density ($g\ cm^{-3}$), ' SOC_{conc} ' is total C (%), 'D' is thickness of the soil layer (cm), and 'SF' is slope factor. The values for total C, total N, and C stocks are reported using the sum of <2 mm and >2 mm soil fractions. Values for total P, Bray P (sequential extraction 1) and exchangeable cations (K, Ca, Mg, Na) were slope corrected and converted to $kg\ ha^{-1}$. The changes in soil pH, total C ($Mg\ ha^{-1}$), total N ($kg\ ha^{-1}$), C:N ratio, $\delta^{13}C$ [‰], total P ($kg\ ha^{-1}$), Bray P 155 ($kg\ ha^{-1}$), total bulk density ($g\ cm^{-3}$), and exchangeable cations K, Ca, Mg, and Na ($kg\ ha^{-1}$) with soil depth were tested for

significance using non-parametric Friedman's tests with soil core transect position as a blocking variable. Post hoc tests were performed using pairwise Wilcoxon rank sum tests with Bonferroni correction.

To calculate differences in the allocation of C stocks down each soil profile, the proportion of C (Mg ha⁻¹) allocated to each depth increment was calculated relative to the sum of total C (Mg ha⁻¹) for each sample core. Differences in 16S and ITS rRNA 160 copy number with depth were tested for significance using Kruskal Wallis chi-squared, with post hoc testing performed using Dunn's test with Bonferroni's adjustment. To estimate the allocation patterns of microbial DNA abundance down the soil profile, the proportion (%) of 16S and ITS rRNA copy numbers allocated to each depth increment were calculated relative to the total sum of the soil core.

2.6.1 Microbial diversity analysis

165 Base calling and demultiplexing of sequencing libraries to per-sample fastQ files was performed using Illumina's bcl2fastq software (version 2.20.0.422). The DADA2 version 1.18 workflow (Callahan et al., 2016) was used to process paired end fastQ files into amplicon sequence variants (ASVs). Briefly, forward and reverse reads were quality filtered, trimmed and denoised before being merged into ASVs. Chimeric ASVs were removed, and taxonomies were assigned to ASVs using the Ribosomal Database Project (RDP) Classifier (Wang et al., 2007) and the UNITE (Abarenkov et al., 2021) databases. After 170 DADA2 processing, $74.92 \pm 5.60\%$ of 16S rRNA input reads and $44.46 \pm 14.35\%$ of ITS rRNA input reads were retained. Following DADA2 processing, ASV tables were filtered to remove unidentified phyla, unwanted phyla (i.e. Cyanobacteria/Chloroplasts), and singletons. For the 16S rRNA dataset, ASVs which had a higher average count in NTC samples than eDNA samples were removed. Rarefaction curves showing ASV richness by depth increment and PCR type can be seen in Figures A3 and A4. Following the removal of samples with low ASV counts, ASV tables were rarefied to even 175 sampling depth prior to analysis (16S rRNA: 11613 ASVs per sample, ITS rRNA: 10101 ASVs per sample).

Microbial alpha and beta diversity analyses were calculated on rarefied ASV tables using the R packages phyloseq (McMurdie and Holmes, 2013) and vegan (Oksanen et al., 2020). Changes in alpha diversity with depth were tested for statistical 180 significance using Kruskal Wallis chi-squared tests as described previously. Pairwise Spearman's correlation tests with Bonferroni adjustment were used to correlate alpha diversity values with soil chemical parameters using psych R (Revelle, 2021). Bray-Curtis distance matrices were calculated to measure community dissimilarity and ordinated using non-metric multidimensional scaling (NMDS). Differences in community dissimilarity by depth were tested for significance using PERMANOVA, and pairwise differences tested using pairwiseAdonis R with Bonferroni adjustment (Arbizu, 2017). For both alpha and beta diversity analyses, the impacts of transect sampling position and nested vs single PCR were tested for significance. Mantel tests were used to correlate Euclidean distance matrices of soil chemical properties to Bray-Curtis 185 matrices of microbial community composition. Venn diagrams were produced to show the proportion (%) shared vs unique ASVs between depth increments using MicEco R (Russel, 2021).

Analysis of Compositions of Microbiomes with Bias Correction (ANCOM-BC; Lin and Peddada, 2020) was used identify microbial taxa which had a significant log-fold change between topsoil (0 to 30 cm) and subsoil layers (30 to 100 cm).

Hierarchical clustering was performed on Euclidean distances of log-adjusted abundances, using the average linkage method
190 (hclust R). Dendograms were constructed using ggtree (Yu et al., 2017) to visualise the hierarchical clustering patterns of microbial orders based on their log-adjusted abundances. The log-adjusted abundances of microbial taxa obtained from ANCOM-BC analysis were correlated to soil chemical properties using pairwise Spearman's correlation tests with Bonferroni adjustment using psych R (Revelle, 2021). To assess changes in the diversity of high-level 16S rRNA functional genes with soil depth, PICRUSt2 was used to predict MetaCyc pathway abundances (Douglas et al., 2020; Caspi et al., 2018). MetaCyc pathway abundance predictions were analysed in phyloseq R using the same alpha and beta diversity methods as outlined
195 above.

2.6.2 Microbial network analysis

ASV tables were split into samples from topsoil (0 to 30 cm) and subsoil (30 to 100 cm) layers to obtain microbial communities specific to each soil layer. Topsoil and subsoil ASV tables were then filtered to retain only 'core' communities (i.e. those with
200 a total relative abundance of at least 0.05% in a minimum of 3 samples) and then summarised to genus level. SPIEC-EASI networks were constructed using the Meinshausen–Buhlmann (MB) neighbourhood algorithm in SpiecEasi R (Kurtz et al., 2015). Networks were visualised using igraph R (Csárdi and Nepusz, 2006) and network statistics were calculated using Cytoscape 3.8.2 (Shannon et al., 2003). Significant differences ($p < 0.05$) in network statistics between topsoil and subsoil communities were tested using Wilcoxon signed rank tests (Mundra et al., 2021). Descriptions of these network
205 statistics can be found in the Supplementary Methods.

3 Results

3.1 Soil chemistry, C stocks, and microbial DNA abundance

Total C (Mg ha^{-1}), total N (kg ha^{-1}), total P (kg ha^{-1}), C:N ratio, and exchangeable cations (K, Ca, Mg, and Na; kg ha^{-1}) significantly declined with soil depth ($p < 0.05$). Soil pH and bulk density (g cm^{-3}) significantly increased with soil depth ($p <$
210 0.05). Results of soil chemical analyses and the corresponding statistical tests are presented in Table A1 and A2.

The average soil C stock of the 1 m soil cores extracted from Puruki Forest was $99.71 \pm 28.78 \text{ Mg ha}^{-1}$ C. The average soil C stock allocated to the coarse ($>2 \text{ mm}$) soil fraction was $1.88 \pm 1.92 \text{ Mg ha}^{-1}$ of C. The amount of soil C stock allocated to the coarse soil fraction did not vary by soil depth increment (ANOVA: F-value = 1.58; $p > 0.05$).

On average, $34.58 \pm 10.25\%$ of the soil C stock was allocated to the 30 to 100 cm (subsoil) layer (Figure 1; Table A3). The
215 proportion of soil C stock allocated to the subsoil varied across the soil cores, ranging from 46.60% to 16.21%. On average, $33.45 \pm 10.92\%$ of fungal DNA and $49.11 \pm 4.82\%$ of bacterial DNA was allocated to the subsoil layers past 30cm depth (Figure 1; Tables A3 and A4). Thus, the allocation patterns of soil C with depth corresponded well to the distribution of bacterial and fungal DNA with depth.

3.2 $\delta^{13}\text{C}$ and ^{14}C natural abundance measurements

220 Overall, $\delta^{13}\text{C}$ [%] significantly increased by 1.58‰ (p < 0.05; Table A1) between depth increments of 0 to 10 and 90 to 100 cm. However, between soil depths of 70 to 90 cm the enrichment of ^{13}C was lower than the rest of the subsoil (Figure 2). Values for ^{14}C [%] and CRA [yBP] of SOC declined with depth (Figure 2; Table A1). The age of SOC steadily increased with depth and reached a mean age of 1570.83 ± 316.28 yBP in the deepest soil layers of 90 to 100 cm.

3.3 Changes in microbial diversity, abundance and composition with depth

225 The richness, diversity, and evenness of fungal and bacterial communities significantly declined with depth (p < 0.05; Figure 3; Table A6 and A7). The same trends were evident for the predicted abundances of bacterial functional genes with depth (Table A7). Transect position had no relationship to bacterial alpha diversity, however fungal evenness did vary across sampling location (Table A7). The DNA abundance of bacteria and fungi significantly declined with soil depth (Figure 3; Table A7) but were unaffected by transect position. Most of the significant differences in alpha diversity and DNA abundance 230 occurred between the upper 0 to 20 cm depth increment and the rest of the soil; few significant pairwise differences were evident among soil layers sampled below 30 cm (Figures A5 to A8). When tested using pairwise Spearman's rank correlations (Figure 4), microbial alpha diversity and abundance were strongly positively correlated to total C, total N, total P, C:N ratio, and ^{14}C (rho > 0.77; p < 0.05). Soil pH was strongly negatively correlated to microbial alpha diversity and abundance (rho > -0.85; p < 0.05). $\delta^{13}\text{C}$ was strongly negatively correlated to fungal richness (rho = -0.85, p < 0.05), and bulk density (g cm⁻³) 235 was strongly negatively correlated to bacterial abundance (rho = -0.90, p < 0.05).

Bacterial (PERMANOVA: $R^2 = 0.21$, p < 0.001) and fungal ($R^2 = 0.26$, p < 0.001) community composition varied significantly between depth increments (Figure 5). Pairwise adonis tests identified that the community composition of soils between 0 to 30 cm contributed to the majority of significant differences between groups, with the differences in microbial composition 240 between soil increments past 30 cm being non-significant (Figure A9). The composition of bacterial and fungal communities significantly differed by sampling transect position (bacteria: $R^2 = 0.13$, p < 0.001; fungi: $R^2 = 0.04$, p < 0.001). However, this accounted for less variation in community composition than soil depth. The composition of bacterial functional genes was significantly different between soil depth increments ($R^2 = 0.34$, p < 0.001; Figure A10).

Mantel tests identified that ^{14}C ($R = 0.38$, p < 0.001), C:N ratio ($R = 0.18$, p < 0.05), bulk density ($R = 0.20$, p < 0.05), Total P ($R = 0.16$, p < 0.001), $\delta^{13}\text{C}$ ($R = 0.13$, p < 0.05), total N ($R = 0.13$, p < 0.05), and exchangeable Ca ($R = 0.12$, p < 0.01) shared 245 a significant but weak correlation to bacterial community composition. Variables that shared a significant but weak correlation to fungal community composition included ^{14}C ($R = 0.32$, p < 0.001), $\delta^{13}\text{C}$ ($R = 0.19$, p < 0.01), total P ($R = 0.19$, p < 0.01), total N ($R = 0.17$, p < 0.01), total C ($R = 0.14$, p < 0.05), and exch. Ca ($R = 0.21$, p < 0.01). Furthermore, total N ($R = 0.17$, p < 0.01), total P ($R = 0.17$, p < 0.01), exchangeable Ca ($R = 0.13$, p < 0.01), bulk density ($R = 0.12$, p < 0.05), $\delta^{13}\text{C}$ ($R = 0.18$, p < 0.01), and ^{14}C ($R = 0.38$, p < 0.001) had a significant but weak correlation to bacterial functional genes.

250 3.5 Microbial taxonomic responses to soil depth

Only 9% of bacterial ASVs and 2% of fungal ASVs were present in all depth increments down the entire soil profile (Figure A11). Upper depth increments (0 to 20 cm) had the highest number of unique bacterial (20%) and fungal (32%) ASVs, suggesting that these upper layers supported a greater range of unique bacterial and fungal taxa than the lower depths. Less than 3% of bacterial ASVs and 1% of fungal ASVs were found to be unique within depth increments from the 40 to 100 cm 255 soil layer; suggesting that subsoils did not harbour vastly unique or distinctive microbial communities from those of topsoil layers.

Archaeal taxa belonging to Thermoplasmata, Desulfurococcales, Thermoprotei, Woesearchaeota incertae sedis (AR15, AR18, AR16, AR20), Euryarchaeota, Candidatus Aenigmarchaeum, and Thermoproteales exhibited significant positive log-fold changes with depth (Figure 6). Furthermore, bacterial taxa belonging to Acidobacteria (e.g. *Bryobacter*, Gp20, Gp18, Gp25, 260 Gp19, Gp6, *Acidicapsa*), Elusimicrobia (*Blastocatella*, *Candidatus Endomicrobium*), Planctomycetes (Phycisphaerales, Tepidisphaerales, Phycisphaerae), Firmicutes (Lactobacillales, Clostridia, Thermoanaerobacterales), Betaproteobacteria (Neisseriales, Ferritrophicales, Hydrogenophilales, Methylophilales) and Armatimonadetes (Gp2, Fimbriimonadetes) exhibited a positive log-fold change in subsoils (Figure 6). Fungal taxa which exhibited a positive log-fold change in subsoils (Figure 6) included Calcarisporiellomycota, Exobasidiomycetes (Entylomatales), Sordariomycetes (Microascales, 265 Trichosphaerales, Annulatascales, Ophiostomatales), Agaricomycetes GS29, Sareomycetes (Sareales), Orbiliomycetes (Orbiliales), Malasseziomycetes (Malasseziales), and Kickxellomycetes (Kickxellales and GS29).

In contrast, bacterial taxa which had significantly negative log-fold change in subsoils (Figure 6) included Chlamydiae (Chlamydiales), Bacteroidetes (Sphingobacteriales, Cytophagales), Acidobacteria (*Edaphobacter*, *Candidatus Solibacter*, *Candidatus Koribacter*, Gp5, Gp16, Gp1, *Terriglobus*), Gammaproteobacteria (Chromatiales), Firmicutes (Clostridiales, 270 Bacillales), Gemmatimonadetes (Gemmatimonadales), Verrucomicrobia (Subdivision 3, *Spartobacteria*), Chloroflexi, Latescibacteria, and Actinobacteria (Ktedonobacterales, Actinomycetales, Gaiellales). The fungal phyla Mucoromycota, Rozellomycota, Mortierellomycota, and Glomeromycota exhibited large negative log-fold change values in subsoils, with members of the classes Tremellomycetes (e.g. Tremellales, Filobasidiales, Trichosporonales), Umbelopsidomycetes (Umbelopsidales), Agaricomycetes (Thelephorales, Boletales), Leotiomycetes (Helotiales, Thelebolales), Sordariomycetes 275 (Xylariales, Chaetosphaerales, Sordariales) and Microbotryomycetes exhibiting strong negative responses to increasing soil depth (Figure 6). More detailed outputs of the ANCOM-BC analysis are presented in Table A8 to A13.

When correlating the abundance of microbial taxa to soil chemical properties, the microbial phyla Bacteroidetes, Chlamydiae, Chloroflexi, Gemmatimonadetes, Mortierellomycota, and Mucoromycota were strongly correlated (Spearman rho > 0.7, p < 0.05) with ¹⁴C abundance (Table A14). Furthermore, of all the soil chemical properties measured, radiocarbon ¹⁴C abundance 280 exhibited the greatest number of strong, significant correlations with the abundances of taxonomic groups (Table A14).

3.6 Structural changes in the soil microbiome with depth

The average node degree and neighbourhood connectivity of topsoil interkingdom networks was significantly than that of subsoils. In contrast, the average shortest path length and clustering coefficient was significantly higher in subsoil interkingdom networks than topsoil interkingdom networks (Figure A12; Table A15). Compared to subsoils, the topsoil interkingdom network had a more connected structure with a greater degree of co-occurrences between genera. For both topsoil and subsoil interkingdom networks, bacterial genera were the dominant community members compared with fungi and archaea (Figure 285 7). Networks of fungal-only topsoil communities had a significantly ($p < 0.05$) higher node degree, neighbourhood connectivity, average shortest path length, and betweenness centrality than fungal-only subsoil networks (Figure A12; Table A15). For prokaryote-only networks (i.e. bacteria and archaea), the average node degree and average shortest path length was 290 significantly higher in the topsoil than subsoil network ($p < 0.05$; Table A15). The fungal-only subsoil network exhibited a sparse structure, with 80.65% of nodes being single nodes i.e. they shared no co-occurrence with any other node (versus 30.34% in the fungal topsoil network). In prokaryote-only networks, single nodes compromised 7.87% of nodes in subsoils and 1.18% of nodes in topsoils. In all of the networks, there was a greater proportion of positive edges (average 70.41%) than negative edges (29.59%) connecting the nodes (Table A15).

295 4.0 Discussion

4.1 Changes in soil C quantity, stabilisation and age with depth

Previous research has identified large stores of unaccounted C stocks located in subsoil layers below 30 cm (Balesdent et al., 2018; Gonzalez et al., 2018; Ross et al., 2020). Our research identified that within Puruki Forest, 35% of soil C stocks were allocated to the subsoil layers below 30 cm. Within our sampling site, subsoil C storage patterns were highly variable and 300 ranged from 19 to 46% of total C stocks. Previously, Oliver et al. (2004) remarked upon the large variability in soil C storage patterns across Puruki Forest, reporting average C stocks of 143 Mg ha^{-1} to 1 m soil depth; values which are higher than observed in our study (99.71 Mg ha^{-1}). High variability in subsoil C storage within Puruki Forest may be a signature of the natural textural and structural variation observed in the pumice soils (Silver et al., 2000; Telles et al., 2003). Furthermore, this variability may be an artefact of Puruki's previous land use history (native forest > pasture > plantation) and the harvesting 305 disturbances associated with historical management practices (Beets et al., 2002; Garrett et al., 2021; Rijkse and Bell, 1974). High variability in soil C stocks across a relatively short spatial distance reaffirms previous research that attributes soil-carbon variability to much of the uncertainty in our ability to quantify subsoil C stocks (Ross et al., 2020). Soils are a significant contributor to the total C sequestration capacity of Puruki Forest and can hold 38% of total planted forest C stocks at end of 310 forest rotation (Garrett et al., 2021). It is important to consider that this study was performed across a small-spatial scale and soil samples were obtained from 10 soil cores extracted along one transect within Puruki Forest. Given the high variability in

soil C values observed in our data, we recommend that future studies perform soil sampling at a higher replication level, with soil cores extracted over a larger spatial extent within the study area under investigation.

We observed an overall enrichment of soil $\delta^{13}\text{C}$ with depth which aligns with previous research (Garten, 2011; Wang et al., 2018). However, this was not a clear linear enrichment and $\delta^{13}\text{C}$ was highly variable between depths of 70 to 90cm. This 315 corresponded to the high structural variability in our soil cores, as there were layers of coarse pumice material (Taupo lapilli) present throughout the subsoil horizons below 50cm (Froggatt, 1981; Rijkse and Bell, 1974). Wynn et al. (2005) identified soil texture as an important factor governing soil $\delta^{13}\text{C}$ enrichment, with finer textured soils being associated with a greater degree of $\delta^{13}\text{C}$ enrichment with soil depth than coarse textured soils. As discussed, Puruki Forest was once formerly covered by native forest prior to being converted to pasture and then planted forest (Beets and Brownlie, 1987). Thus, variability in 320 soil $\delta^{13}\text{C}$ with depth may be a consequence of previous disturbances from land management practices which caused a mixing of topsoil and subsoil layers (Oliver et al., 2004). Down to 1 m soil depth, ^{14}C abundance declined by 229 ‰, which is lower than the median global decline of 502‰ (Mathieu et al., 2015). However, the mean radiocarbon age of our deepest soil layers (~1570 yBP) correspond well to the age of the soil parent materials. Soil parent materials were dominated by the Taupo 325 eruption and this can be directly observed by the layers of Taupo lapilli on Waimihia, Rotoma, Waiohau and Rotorua ash beds present in several of our subsoils. As these layers of Taupo lapilli have been dated as 1760 ± 80 yBP before 1950 (Rijkse and Bell, 1974), we would not have expected any soil radiocarbon ages to have exceeded this value.

4.2 Soil microbial diversity and abundance changed with soil depth

Although microbial DNA abundance declined with depth, accumulatively subsoils held 49% of bacterial and 33% of fungal DNA abundance which corresponded to values for subsoil C stocks. Soil microorganisms are responsible for the mineralisation 330 of SOC and are influential in determining the formation, composition and persistence of SOC (Domeignoz-Horta et al., 2021; Jansson and Hofmockel, 2020). Although subsoil C is considered more resistant to microbial decomposition (Schmidt et al., 2011), an accumulation of microbial ‘stocks’ in proximity to subsoil C stores presents concerns; particularly given our uncertainty on the effects of climate change on soil microbial activity and C substrate use (Yang et al., 2021). However, the contribution of microbial necromass C to total soil C is known to increase with soil depth (Ni et al., 2020). As our research 335 does not provide information on the viability or activity subsoil microbial DNA, much of the accumulated bacterial and fungal DNA in the subsoil may be non-viable microbial cells. Much like incorporating measures of soil C age and stability when quantifying subsoil C stocks, further research should measure the abundance of subsoil microbial cells which are viable and active, as well as those which are dormant but have the potential to become active under global change. Doing so will help us better investigate the vulnerability of subsoil C stocks to microbial decomposition under climate change.

340 Soil microbial diversity and abundance declined sharply with depth which fits in agreement with previous research findings (Blume et al., 2002; Eilers et al., 2012; Mundra et al., 2021; Rosling et al., 2003). These declines occurred alongside clear shifts in microbial community composition. The magnitude of the depth-driven changes slowed past 30 cm, which marked a clear transitional change between the topsoil-subsoil boundary. Although fungal diversity and DNA abundance were generally

much lower than that of bacteria, patterns in response to depth were consistent across both microbial kingdoms. The changes
345 in microbial diversity and abundance were highly correlated with the concentration (total C %) and radiocarbon age of soil C. These findings support research which has proposed declines in soil C quantity, quality, and availability to be strong drivers of declines in microbial diversity and abundance (Eilers et al., 2012). Due to their proximity to aboveground vegetation, topsoil layers typically receive a wider load and range of fresh C inputs from surface litter and plant roots (Fierer et al., 2003; Spohn et al., 2016). This may explain why soil depths 0 to 20 cm supported the greatest number of unique ASVs (i.e. those which
350 occurred only in that soil layer), with the number of unique ASVs declining sharply with depth.

4.3 Shifts in community co-occurrence patterns with depth

Whilst bacterial diversity and abundance declined sharply with depth, bacterial subsoil communities exhibited relatively minor differences in network structure compared to topsoils. Compared to bacterial communities, subsoil fungal networks exhibited greater structural differences between the topsoil and subsoil. Subsoil fungal networks were almost entirely disconnected and
355 there was no suite of co-occurring fungal genera that characterised the subsoil microbiome. The breakdown in subsoil fungal network structure may be explained simplistically by reduced community size limiting the ability for fungal co-occurrences to establish. Although still in low abundance, the relatively larger bacterial community abundance may have contributed to the lesser effects of soil depth on their co-occurrence patterns compared to fungi. Furthermore, as the properties of soil fungal communities are strongly driven by characteristics of aboveground vegetation (Likulunga et al., 2021; Urbanová et al., 2015),
360 the breakdown in subsoil fungal co-occurrences may due to their increasing physical distance from the surface litter and plant rhizosphere.

4.4 Differential responses of microbial taxa to topsoil vs subsoils

Consistent with previous research, we observed an increased abundance of archaeal taxa in subsoils, mainly the phyla
Euryarchaeota, Crenarchaeota, and Woesearchaeota (Brewer et al., 2019; Eilers et al., 2012; Frey et al., 2021; Hartmann et al.,
365 2009). Proposed reasons for the increased abundance of archaea with depth include their adaptation to chronic energy stress (Valentine, 2007); involvement as ammonia oxidizers in driving autotrophic nitrification in deep soil layers (Eilers et al., 2012); preference as methanogens for anaerobic environments (Feng et al., 2019); and adaptation to nutrient poor environments as slow growing oligotrophs (Turner et al., 2017).

Several representatives of the bacterial phyla Acidobacteria and Firmicutes increased in abundance with depth which may be
370 explained by their tolerance for nutrient limited environments (Bai et al., 2017; Brewer et al., 2019; Frey et al., 2021; Feng et al., 2019; Lladó et al., 2017). However, there were several representatives of Acidobacteria and Firmicutes that also declined with depth, such as *Candidatus Solibacter*, *Candidatus Koribacter* and Clostridiales. Hansel et al. (2008) reported high variability in the distribution of Acidobacteria subdivisions amongst different soil horizons. The broad phylogenetic coverage and ecological diversity of Acidobacteria can make it difficult to infer metabolic and functional adaptations based on their
375 taxonomic position alone (Hansel et al., 2008). Such issues highlight the need to adopt more trait-based approaches when

investigating the microbial taxa that exhibit adaptive responses to soil depth. For example, the large genome size of *Candidatus Solibacter* (Challacombe et al., 2011) may explain its high abundance in surface soils, which have a wide range of C and nutrient inputs and greater exposure to environmental flux (Barberán et al., 2014). Theoretically, soil depth may drive a reduction in microorganisms with large genome sizes, as specialisation becomes more favourable under harsh conditions and 380 maintenance of a larger genome becomes too energetically costly.

Strong declines in the abundance of Bacteroidetes with depth has been previously reported and attributed to Bacteroidetes' copiotrophic behaviour (Eilers et al., 2012; Feng et al., 2019; Mundra et al., 2021). In our study, the abundance of Bacteroidetes positively correlated with ¹⁴C abundance. This may indicate the phylum's preference for fast-cycling, bioavailable C which typically declines with depth as more chemically resistant, slow-cycling C forms a greater proportion of the C pool (Koarashi 385 et al., 2012; Torn et al., 1997). Another bacterial phylum which declined in abundance with depth, Chlamydiae, was positively correlated to younger SOC ages. Chlamydiae has also been positively associated with lower pH, organic matter content and C:N ratio (Zhalnina et al., 2015; Ma et al., 2021), properties which commonly change with soil depth. The declines in Gemmatimonadetes and Chloroflexi with depth observed in our study is inconsistent with previous research (Bai et al., 2017; Chu et al., 2016; Frey et al., 2021; Li et al., 2020; Seuradge et al., 2016; Zhang et al., 2019). The increased abundance of 390 Gemmatimonadetes' with depth has previously been attributed to their preference for low soil moisture conditions (Debruyne et al., 2011; Frey et al., 2021). However, the highly permeable soils within Puruki Forest exhibit a greater potential for soil moisture to increase with depth, with the subsoil horizons having a high moisture capacity (Beets and Brownlie, 1987; Will and Stone, 1967; Beets and Beets, 2020). Thus, the decline of Gemmatimonadetes with soil depth at Puruki Forest may be due to its preference for low soil moisture conditions. Carteron et al. (2021) observed large shifts in the ratio of saprophytic: 395 mycorrhizal abundance with soil depth, which correlated to changes in soil chemistry. In our study, soil depth was associated with large declines in fungal taxa (i.e. Mucoromycota, Rozellomycota, Mortierellomycota, and Glomeromycota) previously reported in the literature as saprophytic and rhizospheric fungi (Bonfante and Venice, 2020; Hoffmann et al., 2011; Wagner et al., 2013; Yurkov et al., 2016).

5.0 Conclusions

400 The findings of our research address knowledge gaps related to subsoil C dynamics for production forests such Puruki Forest. A considerable proportion (at least 35%) of soil C stocks within Puruki Forest were allocated to the subsoil layers below 30 cm, with this value reaching up to 49% in some soil cores. In the deepest soil layers, the mean C age was 1571 yBP, corresponding closely to the estimated age of soil parent materials. Although there were large declines in bacterial and fungal 405 DNA abundance and diversity with soil depth, the magnitude of these changes slowed past 30 cm depth. This marked a topsoil subsoil transitional boundary in the soil profile. In total, 49% of bacterial and 33% of fungal DNA abundance was allocated to the subsoil. Quantifying the viable activity of this microbial 'biomass' is essential for predicting the vulnerability of subsoil C stocks to microbial decomposition under climate change. Numerous archaeal taxa exhibited an increased abundance in

subsoils, indicating their potential ecological importance in deep soil environments. Furthermore, numerous fungal and bacterial taxa exhibited significant differential abundances between topsoil and subsoil layers. This supports the notion that 410 subsoil environments act as an environmental filter; with the vertical distribution of soil microorganisms reflecting the sharp changes in soil physical and chemical properties with depth.

Author contribution

Alexa K. Byers: Methodology, Formal analysis, Data curation, Writing- Original Draft, Visualization. Loretta G. Garrett: Methodology, Writing- Review & Editing, Supervision, Project administration. Charlotte Armstrong: Methodology. Fiona 415 Dean: Methodology, Resources. Steve A. Wakelin: Conceptualization, Writing - Review & Editing, Supervision, Project administration, Funding acquisition.

Code/Data availability

The R code and datasets generated during this current study are available from the corresponding author on reasonable request.

Competing interests

420 The authors have no competing interests to declare.

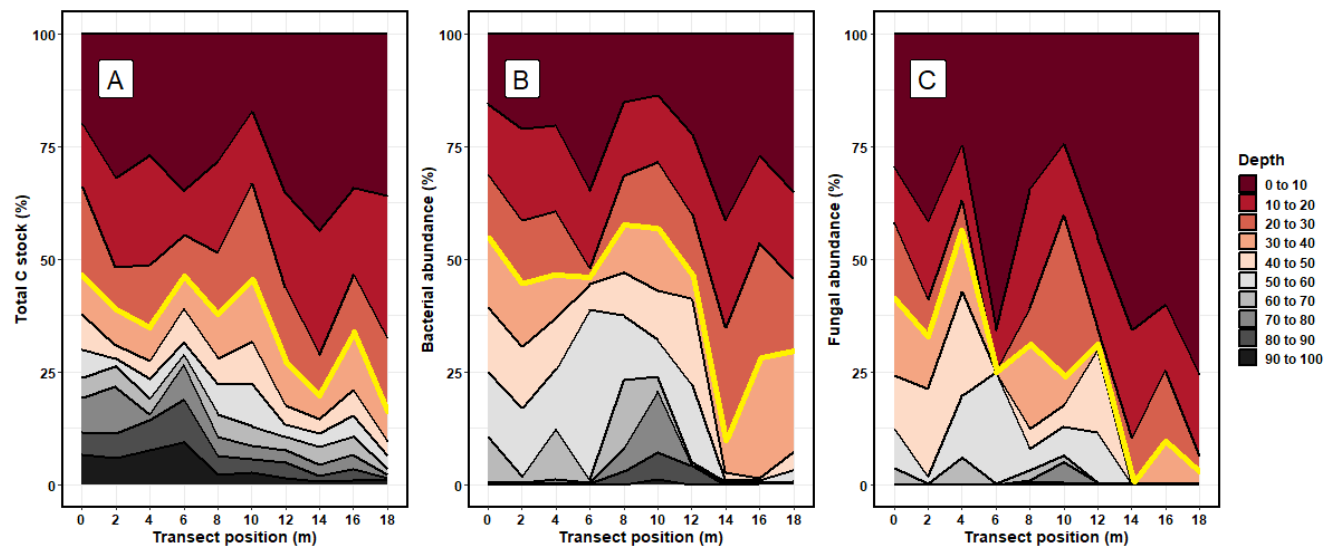
Acknowledgements

Thank you to all the staff at Scion analytical laboratory services (Scion, NZ), Angela Wakelin (Scion, NZ), Stephen Pearce (Scion, NZ), Jeff Hatten (Oregon State University, US), and Katherine Heckman (U.S Department of Agriculture, US) for your invaluable contributions towards this research project.

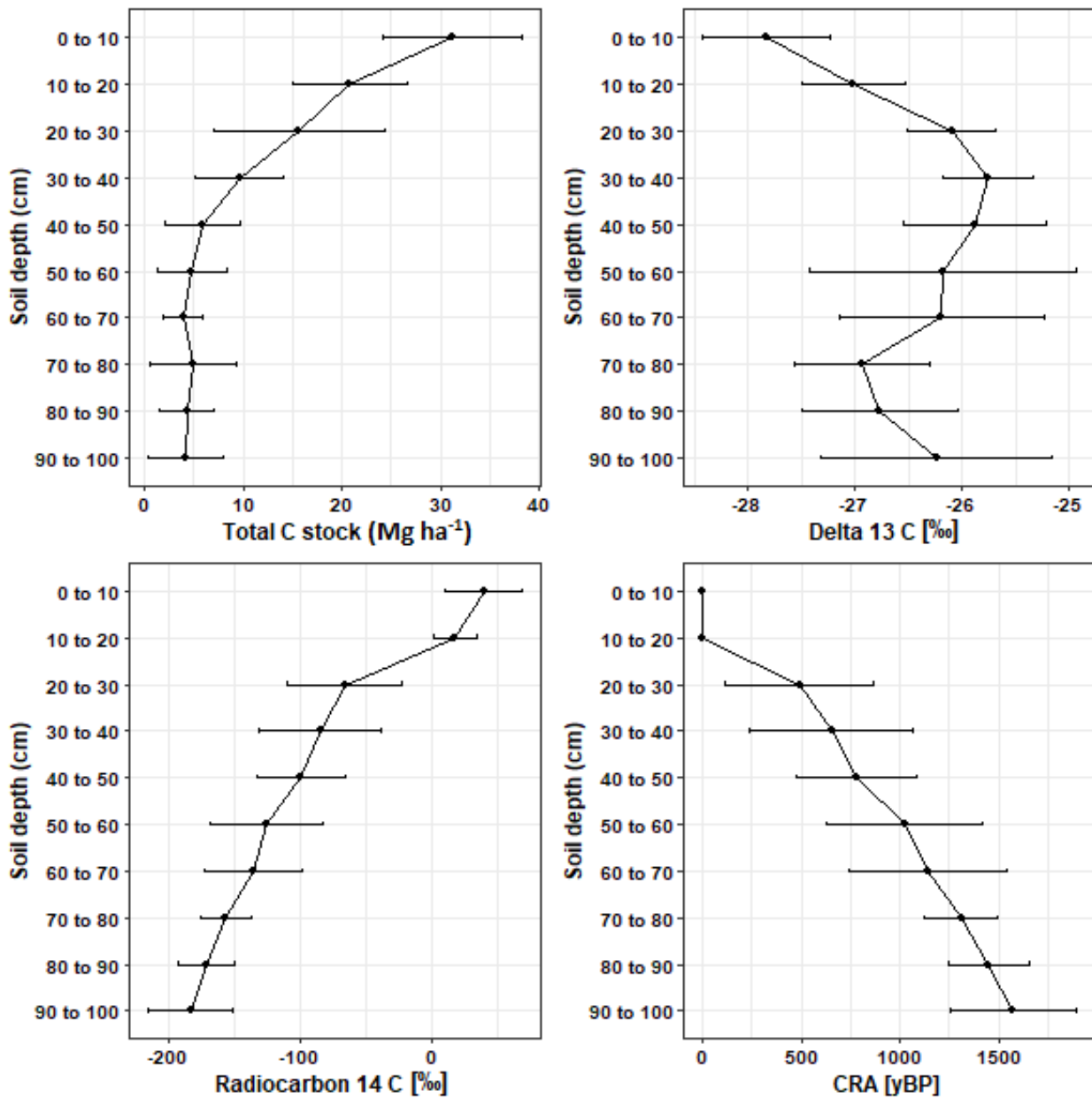
425 Funding

Funding for this research came from New Zealand Ministry of Business, Innovation & Employment (MBIE) Strategic Science Investment Fund held by Scion (C04X1703).

Figures and Tables



430 **Figure 1.** The relative proportion (%) of (a) total carbon stocks ($C \text{ Mg ha}^{-1}$), (b) bacterial DNA abundance and (c) fungal DNA abundance allocated to each depth increment. The values for total C stocks are reported using the sum of $<2 \text{ mm}$ and $>2 \text{ mm}$ soil fractions. The transect position (m) shows where each soil core was extracted from along the sampling transect. Red line shows typical 'cut off' point of topsoil subsoil boundary, where measures below 30 cm are rarely taken.



435 Figure 2. The mean \pm SD changes in total C stock (Mg ha^{-1}), $\delta^{13}\text{C}$ [‰], $\Delta^{14}\text{C}$ [‰] and conventional radiocarbon age (CRA) [yBP] with soil depth.

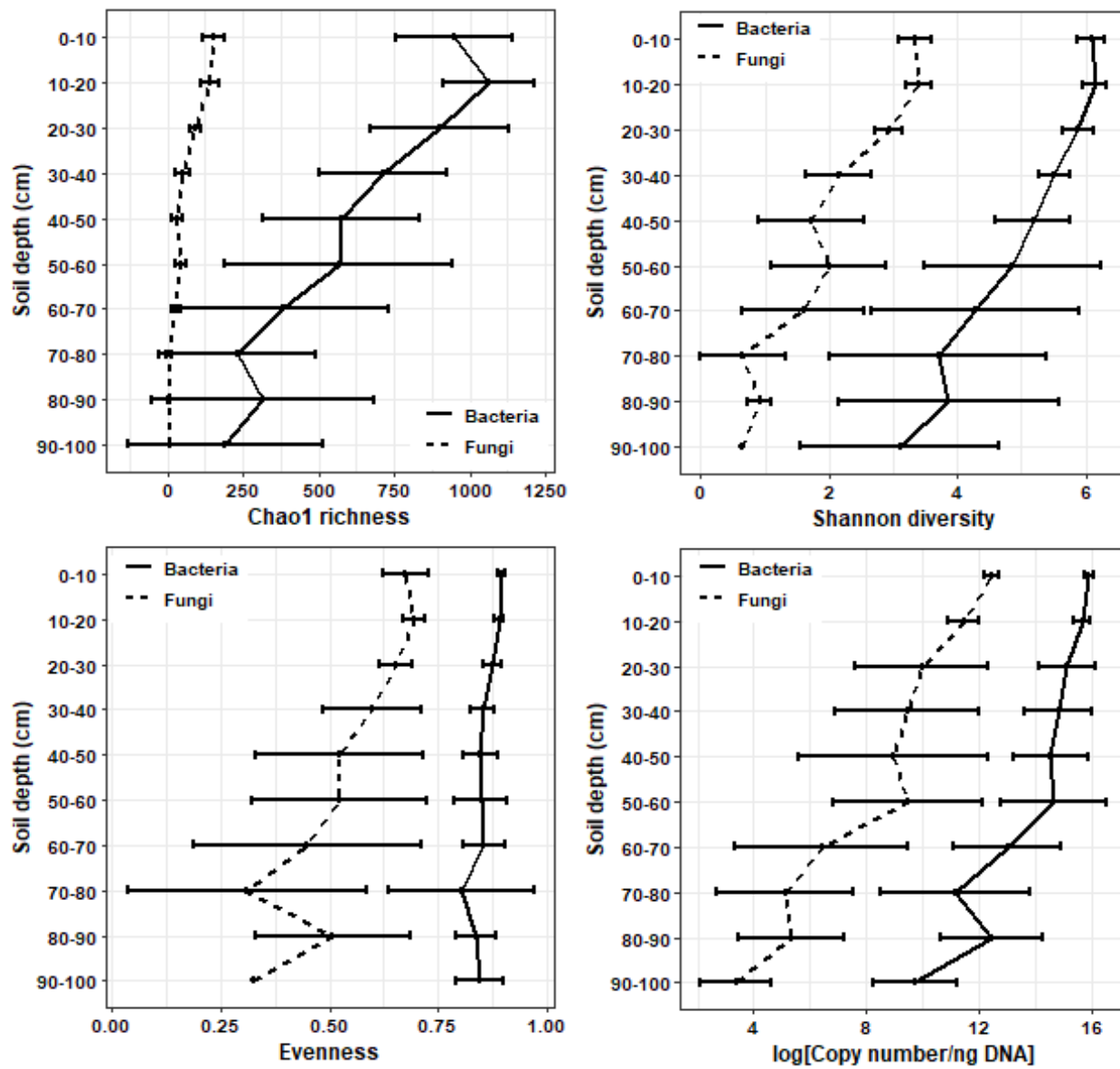
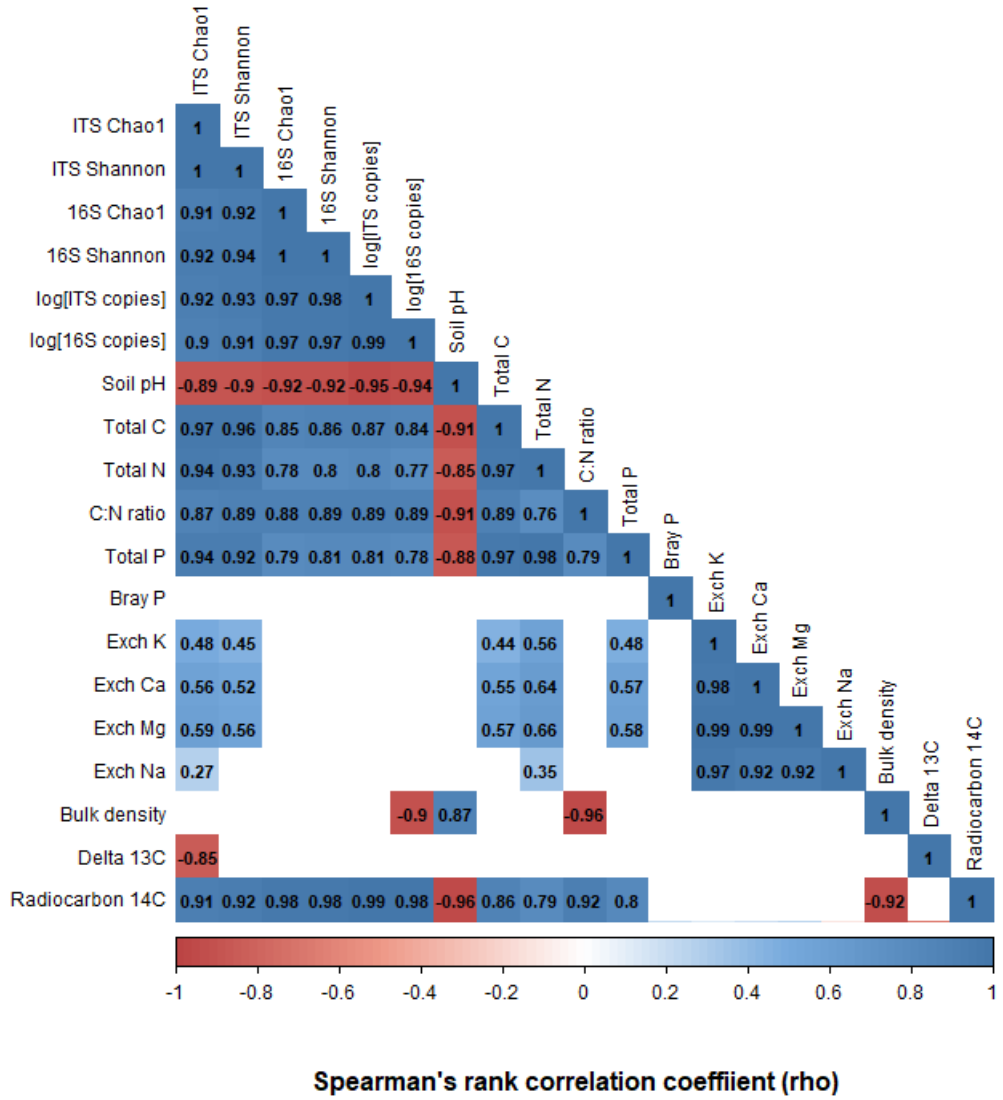


Figure 3. The mean \pm SD changes in microbial richness, Shannon diversity, Pielou's evenness, and 16S/ITS rRNA copy number with soil depth.



440

Figure 4. Pairwise Spearman's correlation matrix showing the correlation between microbial richness, diversity, DNA abundance and soil chemical properties. Blank cells indicate non-significant ($p > 0.05$) correlations.

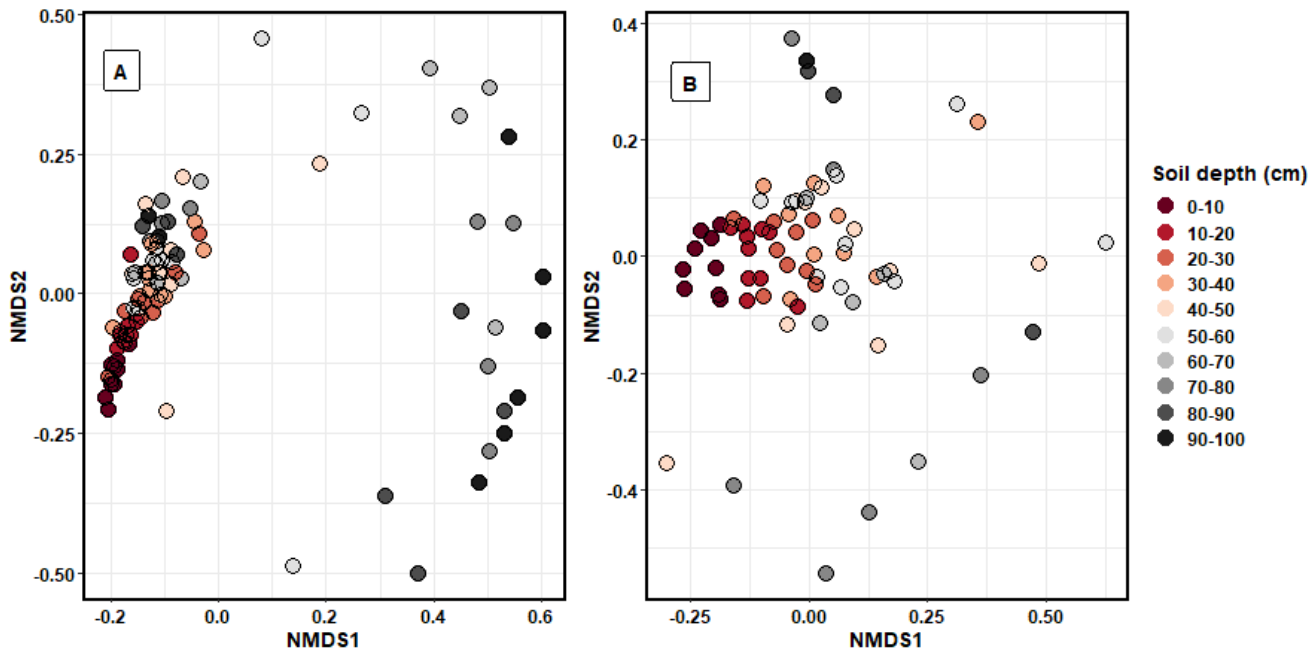


Figure 5. NMDS ordination plots calculated using Bray Curtis dissimilarity matrices showing the differences in (A) bacterial and (B) fungal community composition between the different soil depth increments.

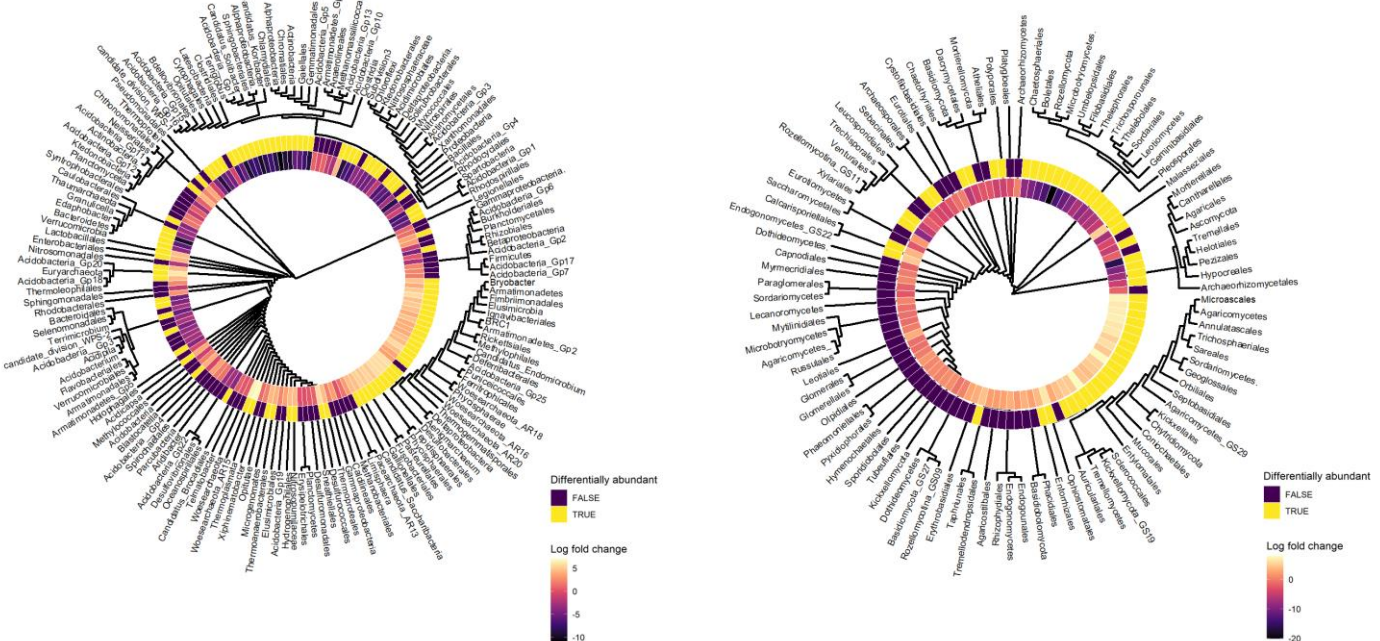
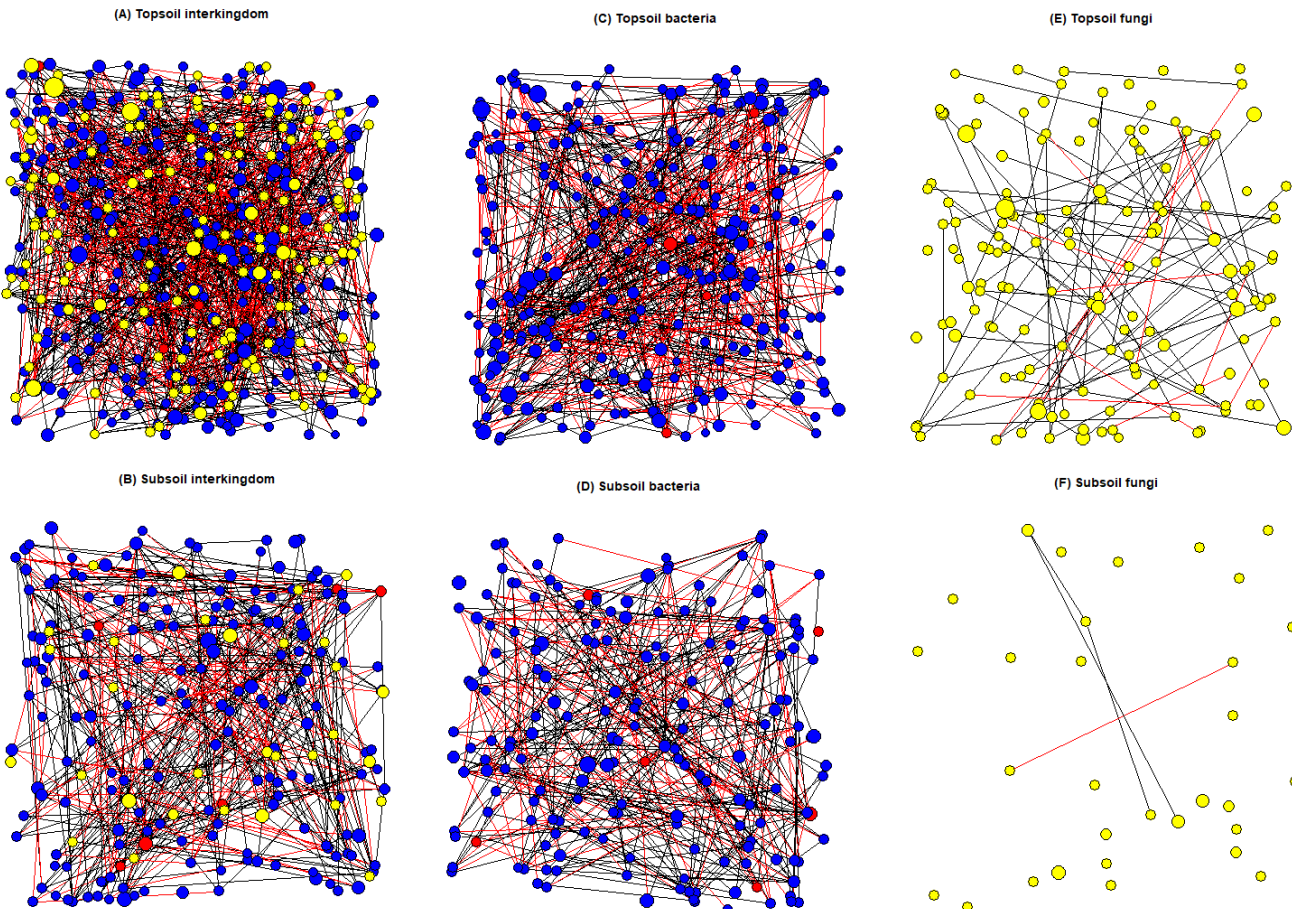


Figure 6. Cluster dendograms of bacterial and fungal orders based on their bias-adjusted abundances (ANCOM-BC analysis). Hierarchical clustering was performed on Euclidean distances of bias-adjusted abundances using the average linkage method. The log fold change (LFC) value of each taxa between topsoil and subsoil is displayed. Taxa with positive LFC values were higher in

450 subsoils and taxa with negative LFC values were lower in subsoils. The statistical significance of each taxa's differential abundance
 between topsoil and subsoil is displayed, with TRUE = $p < 0.05$ and FALSE = $p > 0.05$.



455
 Figure 7. SPIEC-EASI networks constructed on core microbial genera associated with topsoil (0 to 30cm depth) and subsoil (30 to
 100cm depth) layers. Node size represents each genus' normalized (centred log ratio) mean abundance. Blue nodes represent
 bacterial genera, red nodes represent archaeal genera, and yellow nodes represent fungal genera. Positive edge weights are shown by black lines connecting nodes, negative edge weights are shown by red lines connecting nodes.

References

Abarenkov, K., Zirk, A., Piirmann, T., Pöhönen, R., Ivanov, F., Nilsson, R. H., and Kõljalg, U.: UNITE general FASTA release
 for Fungi, doi:10.15156/BIO/1280049, 2021.

460 Arbizu, P. M.: pairwiseAdonis: Pairwise Multilevel Comparison using Adonis. (R package version 0.0.1.), 2017.

Bai, R., Wang, J.-T., Deng, Y., He, J.-Z., Feng, K., and Zhang, L.-M.: Microbial Community and Functional Structure
 Significantly Varied among Distinct Types of Paddy Soils But Responded Differently along Gradients of Soil Depth Layers,
 Front Microbiol, 8, doi:10.3389/fmicb.2017.00945, 2017.

Balesdent, J., Basile-Doelsch, I., Chadoeuf, J., Cornu, S., Derrien, D., Fekiacova, Z., and Hatté, C.: Atmosphere–soil carbon
 465 transfer as a function of soil depth, Nature, 559, 599–602, doi:10.1038/s41586-018-0328-3, 2018.

Barberán, A., Ramirez, K. S., Leff, J. W., Bradford, M. A., Wall, D. H., and Fierer, N.: Why are some microbes more ubiquitous than others? Predicting the habitat breadth of soil bacteria, *Ecology Letters*, 17, 794-802, doi:10.1111/ele.12282, 2014.

Batjes, N. H.: Total carbon and nitrogen in the soils of the world, *European journal of soil science*, 47, 151-163, 1996.

Beets, P. and Brownlie, R.: Puruki experimental catchment: site, climate, forest management, and research, *New Zealand Journal of Forestry Science*, 17, 137-160, 1987.

Beets, P. N. and Beets, J. M.: Soil water storage changes in a small headwater catchment in the central North Island of New Zealand following afforestation with *Pinus radiata*, *Forest Ecology and Management*, 462, 117967, doi:10.1016/j.foreco.2020.117967, 2020.

Beets, P., Oliver, G., and Clinton, P.: Soil carbon protection in podocarp/hardwood forest, and effects of conversion to pasture and exotic pine forest, *Environmental pollution*, 116, 63-73, doi:10.1016/S0269-7491(01)00248-2, 2002.

Blakemore, L. C., Searle, P. L., and Daly, B. K.: Methods for chemical analysis of soils, *Department of Scientific and Industrial Research, New Zealand*, 1977.

Blume, E., Bischoff, M., Reichert, J., Moorman, T., Konopka, A., and Turco, R.: Surface and subsurface microbial biomass, community structure and metabolic activity as a function of soil depth and season, *Applied Soil Ecology*, 20, 171-181, 2002.

Bokulich, N. A. and Mills, D. A.: Improved Selection of Internal Transcribed Spacer-Specific Primers Enables Quantitative, Ultra-High-Throughput Profiling of Fungal Communities, *Applied and Environmental Microbiology*, 79, 2519-2526, doi:10.1128/AEM.03870-12, 2013.

Bonfante, P. and Venice, F.: Mucoromycota: going to the roots of plant-interacting fungi, *Fungal Biology Reviews*, 34, 100-113, doi:10.1016/j.fbr.2019.12.003, 2020.

Bray, R. H. and Kurtz, L. T.: Determination of total, organic, and available forms of phosphorus in soils, *Soil Science*, 59, 1945.

Brewer, T. E., Aronson, E. L., Arogyaswamy, K., Billings, S. A., Bothoff, J. K., Campbell, A. N., Dove, N. C., Fairbanks, D., Gallery, R. E., Hart, S. C., Kaye, J., King, G., Logan, G., Lohse, K. A., Maltz, M. R., Mayorga, E., O'Neill, C., Owens, S. M., Packman, A., Pett-Ridge, J., Plante, A. F., Richter, D. D., Silver, W. L., Yang, W. H., and Fierer, N.: Ecological and Genomic Attributes of Novel Bacterial Taxa That Thrive in Subsurface Soil Horizons, *mBio*, 10, e01318-01319, doi:10.1128/mBio.01318-19, 2019.

Brownlie, R. and Kelliher, F.: Puruki forest climate, *FRI bulletin-Forest Research Institute, New Zealand Forest Service*, 1989.

Callahan, B. J., McMurdie, P. J., Rosen, M. J., Han, A. W., Johnson, A. J. A., and Holmes, S. P.: DADA2: High-resolution sample inference from Illumina amplicon data, *Nature Methods*, 13, 581-583, doi:10.1038/nmeth.3869, 2016.

Caporaso, J. G., Lauber, C. L., Walters, W. A., Berg-Lyons, D., Huntley, J., Fierer, N., Owens, S. M., Betley, J., Fraser, L., and Bauer, M.: Ultra-high-throughput microbial community analysis on the Illumina HiSeq and MiSeq platforms, *The ISME journal*, 6, 1621-1624, 2012.

Carteron, A., Beigas, M., Joly, S., Turner, B. L., and Laliberté, E.: Temperate Forests Dominated by Arbuscular or Ectomycorrhizal Fungi Are Characterized by Strong Shifts from Saprotrrophic to Mycorrhizal Fungi with Increasing Soil Depth, *Microbial Ecology*, 82, 377-390, doi:10.1007/s00248-020-01540-7, 2021.

Caspi, R., Billington, R., Fulcher, C. A., Keseler, I. M., Kothari, A., Krummenacker, M., Latendresse, M., Midford, P. E., Ong, Q., Ong, W. K., Paley, S., Subhraveti, P., and Karp, P. D.: The MetaCyc database of metabolic pathways and enzymes, *Nucleic Acids Res*, 46, D633-d639, doi:10.1093/nar/gkx935, 2018.

Chabbi, A., Kögel-Knabner, I., and Rumpel, C.: Stabilised carbon in subsoil horizons is located in spatially distinct parts of the soil profile, *Soil Biology and Biochemistry*, 41, 256-261, 2009.

Challacombe, J., Eichorst, S., Hauser, L., Land, M., Xie, G., and Kuske, C.: Biological Consequences of Ancient Gene Acquisition and Duplication in the Large Genome of *Candidatus Solibacter usitatus* Ellin6076, *PLoS ONE*, 6, e24882, doi:10.1371/journal.pone.0024882, 2011.

Chu, H., Sun, H., Tripathi, B. M., Adams, J. M., Huang, R., Zhang, Y., and Shi, Y.: Bacterial community dissimilarity between the surface and subsurface soils equals horizontal differences over several kilometers in the western Tibetan Plateau, *Environmental Microbiology*, 18, 1523-1533, doi:10.1111/1462-2920.13236, 2016.

Csárdi, G. and Nepusz, T.: The igraph software package for complex network research,

Curd, E. E., Martiny, J. B., Li, H., and Smith, T. B.: Bacterial diversity is positively correlated with soil heterogeneity, *Ecosphere*, 9, e02079, 2018.

515 DeBruyn, J. M., Nixon, L. T., Fawaz, M. N., Johnson, A. M., and Radosevich, M.: Global Biogeography and Quantitative Seasonal Dynamics of Gemmatimonadetes in Soil, *Applied and Environmental Microbiology*, 77, 6295-6300, doi:10.1128/AEM.05005-11, 2011.

520 Domeignoz-Horta, L. A., Shinfuku, M., Junier, P., Poirier, S., Verrecchia, E., Sebag, D., and DeAngelis, K. M.: Direct evidence for the role of microbial community composition in the formation of soil organic matter composition and persistence, *ISME Communications*, 1, 64, doi:10.1038/s43705-021-00071-7, 2021.

Douglas, G., Mackay, A., Vibart, R., Dodd, M., McIvor, I., and McKenzie, C.: Soil carbon stocks under grazed pasture and pasture-tree systems, *Sci Total Environ*, 715, 136910, doi:10.1016/j.scitotenv.2020.136910, 2020.

Eilers, K. G., Debenport, S., Anderson, S., and Fierer, N.: Digging deeper to find unique microbial communities: the strong effect of depth on the structure of bacterial and archaeal communities in soil, *Soil Biology and Biochemistry*, 50, 58-65, 2012.

525 Fang, C., Smith, P., Moncrieff, J. B., and Smith, J. U.: Similar response of labile and resistant soil organic matter pools to changes in temperature, *Nature*, 433, 57-59, 2005.

Feng, H., Guo, J., Wang, W., Song, X., and Yu, S.: Soil Depth Determines the Composition and Diversity of Bacterial and Archaeal Communities in a Poplar Plantation, *Forests*, 10, 550, 2019.

530 Fierer, N., Allen, A. S., Schimel, J. P., and Holden, P. A.: Controls on microbial CO₂ production: a comparison of surface and subsurface soil horizons, *Global Change Biology*, 9, 1322-1332, doi:10.1046/j.1365-2486.2003.00663.x, 2003.

Frey, B., Walthert, L., Perez-Mon, C., Stierli, B., Köchli, R., Dharmarajah, A., and Brunner, I.: Deep Soil Layers of Drought-Exposed Forests Harbor Poorly Known Bacterial and Fungal Communities, *Front Microbiol*, 12, doi:10.3389/fmicb.2021.674160, 2021.

535 Froggatt, P. C.: Stratigraphy and nature of Taupo Pumice Formation, *New Zealand Journal of Geology and Geophysics*, 24, 231-248, doi:10.1080/00288306.1981.10422715, 1981.

Garrett, L. G., Wakelin, S. A., Pearce, S. H., Wakelin, S. J., and Barnard, T.: Puruki Experimental Forest - half a century of forestry research, *New Zealand Journal of Forestry*, 66, 3-10, 2021.

Garten, C. T., Hanson, P. J., Todd, D. E., Lu, B. B., Brice, D. J., Lajtha, K., and Michener, R.: Natural 15N-and 13C-abundance as indicators of forest nitrogen status and soil carbon dynamics, *Stable isotopes in ecology and environmental science*, 61, 61-82, 2008.

540 Garten, C. T.: Comparison of forest soil carbon dynamics at five sites along a latitudinal gradient, *Geoderma*, 167-168, 30-40, doi:10.1016/j.geoderma.2011.08.007, 2011.

Gattinger, A., Muller, A., Haeni, M., Skinner, C., Fliessbach, A., Buchmann, N., Mäder, P., Stolze, M., Smith, P., Scialabba, N.E.H. and Niggli, U.: Enhanced topsoil carbon stocks under organic farming. *Proceedings of the National Academy of Sciences*, 109, 18226-18231, doi:10.1073/pnas.120942910, 2012.

545 Gonzalez, Y. N., Bacon, A. R., and Harris, W. G.: A Billion Tons of Unaccounted for Carbon in the Southeastern United States, *Geophysical Research Letters*, 45, 7580-7587, doi:10.1029/2018GL077540, 2018.

Gross, C. D. and Harrison, R. B.: The Case for Digging Deeper: Soil Organic Carbon Storage, Dynamics, and Controls in Our Changing World, *Soil Systems*, 3, doi:10.3390/soilsystems3020028, 2019.

550 Hansel, C. M., Fendorf, S., Jardine, P. M., and Francis, C. A.: Changes in bacterial and archaeal community structure and functional diversity along a geochemically variable soil profile, *Applied and environmental microbiology*, 74, 1620-1633, 2008.

Hao, J., Chai, Y. N., Lopes, L. D., Ordóñez, R. A., Wright, E. E., Archontoulis, S., and Schachtman, D. P.: The Effects of Soil Depth on the Structure of Microbial Communities in Agricultural Soils in Iowa (United States), *Applied and Environmental Microbiology*, 87, e02673-02620, doi:10.1128/AEM.02673-20, 2021.

555 Hartmann, M., Lee, S., Hallam, S. J., and Mohn, W. W.: Bacterial, archaeal and eukaryal community structures throughout soil horizons of harvested and naturally disturbed forest stands, *Environmental Microbiology*, 11, 3045-3062, 2009.

Hewitt, A. E.: New Zealand soil classification, *Landcare research science series*, 2010.

Hoffmann, K., Voigt, K., and Kirk, P.: Mortierellomycotina subphyl. nov., based on multi-gene genealogies, *Mycotaxon*, 115, 353-363, doi:10.5248/115.353, 2011.

Hoggard, M., Vesty, A., Wong, G., Montgomery, J. M., Fourie, C., Douglas, R. G., Biswas, K., and Taylor, M. W.: Characterizing the Human Mycobiota: A Comparison of Small Subunit rRNA, ITS1, ITS2, and Large Subunit rRNA Genomic Targets, *Front Microbiol*, 9, doi:10.3389/fmicb.2018.02208, 2018.

565 Jandl, R., Lindner, M., Vesterdal, L., Bauwens, B., Baritz, R., Hagedorn, F., Johnson, D. W., Minkkinen, K., and Byrne, K. A.: How strongly can forest management influence soil carbon sequestration?, *Geoderma*, 137, 253-268, doi:10.1016/j.geoderma.2006.09.003, 2007.

Jansson, J. K. and Hofmockel, K. S.: Soil microbiomes and climate change, *Nature Reviews Microbiology*, 18, 35-46, 2020.

Jastrow, J. D., Amonette, J. E., and Bailey, V. L.: Mechanisms controlling soil carbon turnover and their potential application for enhancing carbon sequestration, *Climatic Change*, 80, 5-23, doi:10.1007/s10584-006-9178-3, 2007.

570 Jobbágy, E. and Jackson, R.: The Vertical Distribution of Soil Organic Carbon and Its Relation to Climate and Vegetation, *Ecological Applications*, 10, 423-436, doi:10.2307/2641104, 2000.

Jones, H. S., Garrett, L. G., Beets, P. N., Kimberley, M. O., & Oliver, G. R. Impacts of harvest residue management on soil carbon stocks in a plantation forest. *Soil Science Society of America Journal*, 72, 1621-1627, doi:10.2136/sssaj2007.0333, 2008.

575 Koarashi, J., Hockaday, W. C., Masiello, C. A., and Trumbore, S. E.: Dynamics of decadally cycling carbon in subsurface soils, *Journal of Geophysical Research: Biogeosciences*, 117, doi:10.1029/2012JG002034, 2012.

Kurtz, Z. D., Müller, C. L., Miraldi, E. R., Littman, D. R., Blaser, M. J., and Bonneau, R. A.: Sparse and Compositionally Robust Inference of Microbial Ecological Networks, *PLOS Computational Biology*, 11, e1004226, doi:10.1371/journal.pcbi.1004226, 2015.

580 Kuzyakov, Y. and Blagodatskaya, E.: Microbial hotspots and hot moments in soil: Concept & review, *Soil Biology and Biochemistry*, 83, 184-199, doi:10.1016/j.soilbio.2015.01.025, 2015.

Kuzyakov, Y.: Priming effects: Interactions between living and dead organic matter, *Soil Biology and Biochemistry*, 42, 1363-1371, doi:10.1016/j.soilbio.2010.04.003, 2010.

Lal, R.: Soil Carbon Sequestration Impacts on Global Climate Change and Food Security, *Science*, 304, 1623-1627, doi:10.1126/science.1097396, 2004.

585 Li, X., Wang, H., Li, X., Li, X., and Zhang, H.: Distribution characteristics of fungal communities with depth in paddy fields of three soil types in China, *Journal of Microbiology*, 58, 279-287, doi:10.1007/s12275-020-9409-8, 2020.

Likulunga, L. E., Rivera Pérez, C. A., Schneider, D., Daniel, R., and Polle, A.: Tree species composition and soil properties in pure and mixed beech-conifer stands drive soil fungal communities, *Forest Ecology and Management*, 502, 119709, doi:10.1016/j.foreco.2021.119709, 2021.

590 Lin, H. and Peddada, S. D.: Analysis of microbial compositions: a review of normalization and differential abundance analysis, *npj Biofilms and Microbiomes*, 6, 60, doi:10.1038/s41522-020-00160-w, 2020.

Lladó, S., López-Mondéjar, R., and Baldrian, P.: Forest Soil Bacteria: Diversity, Involvement in Ecosystem Processes, and Response to Global Change, *Microbiology and Molecular Biology Reviews*, 81, e00063-00016, doi:10.1128/MMBR.00063-16, 2017.

595 Ma, Y., Feng, C., Wang, Z., Huang, C., Huang, X., Wang, W., Yang, S., Fu, S., and Chen, H. Y. H.: Restoration in degraded subtropical broadleaved forests induces changes in soil bacterial communities, *Global Ecology and Conservation*, 30, e01775, doi:10.1016/j.gecco.2021.e01775, 2021.

Mathieu, J. A., Hatté, C., Balesdent, J., and Parent, É.: Deep soil carbon dynamics are driven more by soil type than by climate: a worldwide meta-analysis of radiocarbon profiles, *Global change biology*, 21, 4278-4292, 2015.

600 McMurdie, P. J. and Holmes, S.: phyloseq: An R Package for Reproducible Interactive Analysis and Graphics of Microbiome Census Data, *PLOS ONE*, 8, e61217, doi:10.1371/journal.pone.0061217, 2013.

Mukul, S. A., Halim, M. A., and Herbohn, J.: Forest carbon stock and fluxes: distribution, biogeochemical cycles, and measurement techniques, *Life on Land, Encyclopedia of the UN Sustainable Development Goals*; Leal Filho, W., Azul, AM, Brandli, L., Lange Salvia, A., Wall, T., Eds, 2020.

605 Mundra, S., Kjonaas, O. J., Morgado, L. N., Krabberod, A. K., Ransedokken, Y., and Kauserud, H.: Soil depth matters: shift in composition and inter-kingdom co-occurrence patterns of microorganisms in forest soils, *FEMS Microbiol Ecol*, 97, doi:10.1093/femsec/fiab022, 2021.

Ni, X., Liao, S., Tan, S., Peng, Y., Wang, D., Yue, K., Wu, F., and Yang, Y.: The vertical distribution and control of microbial necromass carbon in forest soils, *Global Ecology and Biogeography*, 29, 1829-1839, doi:10.1111/geb.13159, 2020.

610 Oksanen, J., Blanchet, G., Friendly, M., Kindt, R., Legendre, P., McGlinn, D., Minchin, P. R., O'Hara, R. B., Simpson, G. L., Solymos, P., Stevens, H. H., Szoecs, E., and Wagner, H.: vegan: Community Ecology Package, 2020.

615 Oliver, G., Beets, P., Garrett, L., Pearce, S. H., Kimberley, M., Ford-Robertson, J. B., and Robertson, K.: Variation in soil carbon in pine plantations and implications for monitoring soil carbon stocks in relation to land-use change and forest site management in New Zealand, *Forest Ecology and Management*, 203, 283-295, doi:10.1016/j.foreco.2004.07.045, 2004.

616 Paul, A., Balesdent, J., and Hatté, C.: 13C-14C relations reveal that soil 13C-depth gradient is linked to historical changes in vegetation 13C, *Plant and Soil*, 447, 305-317, doi:10.1007/s11104-019-04384-4, 2020.

617 Poage, M. A. and Feng, X.: A theoretical analysis of steady state $\delta^{13}\text{C}$ profiles of soil organic matter, *Global Biogeochemical Cycles*, 18, doi:10.1029/2003GB002195, 2004.

618 620 Rayment, G. E. and Lyons, D. J.: *Soil chemical methods: Australasia*, CSIRO publishing 2011.

619 Revelle, W.: *psych: Procedures for Personality and Psychological Research*, 2021.

621 Rijkse, W. C. and Bell, J.: Soils of Purukohukohu IHD Experimental Basin, Rotorua County, North Island, New Zealand, NZ soil survey report, 1974.

622 625 Rosling, A., Landeweert, R., Lindahl, B. D., Larsson, K. H., Kuyper, T. W., Taylor, A. F. S., and Finlay, R. D.: Vertical distribution of ectomycorrhizal fungal taxa in a podzol soil profile, *New Phytologist*, 159, 775-783, doi:10.1046/j.1469-8137.2003.00829.x, 2003.

626 Ross, C. W., Grunwald, S., Vogel, J. G., Markewitz, D., Jokela, E. J., Martin, T. A., Bracho, R., Bacon, A. R., Brungard, C. W., and Xiong, X.: Accounting for two-billion tons of stabilized soil carbon, *Sci Total Environ*, 703, 134615, doi:10.1016/j.scitotenv.2019.134615, 2020.

627 630 Russel, J.: *Russel88/MicEco: v0.9.15 (v0.9.15)*, Zenodo, doi:10.5281/zenodo.4733747, 2021.

628 Schmidt, M. W. I., Torn, M. S., Abiven, S., Dittmar, T., Guggenberger, G., Janssens, I. A., Kleber, M., Kögel-Knabner, I., Lehmann, J., Manning, D. A. C., Nannipieri, P., Rasse, D. P., Weiner, S., and Trumbore, S. E.: Persistence of soil organic matter as an ecosystem property, *Nature*, 478, 49-56, doi:10.1038/nature10386, 2011.

629 635 Seuradge, B. J., Oelbermann, M., and Neufeld, J. D.: Depth-dependent influence of different land-use systems on bacterial biogeography, *FEMS Microbiology Ecology*, 93, doi:10.1093/femsec/fiw239, 2016.

636 Shahsavari, E., Aburto-Medina, A., Taha, M., and Ball, A. S.: A quantitative PCR approach for quantification of functional genes involved in the degradation of polycyclic aromatic hydrocarbons in contaminated soils, *MethodsX*, 3, 205-211, doi:10.1016/j.mex.2016.02.005, 2016.

637 640 Shannon, P., Markiel, A., Ozier, O., Baliga, N. S., Wang, J. T., Ramage, D., Amin, N., Schwikowski, B., and Ideker, T.: *Cytoscape: a software environment for integrated models of biomolecular interaction networks*, *Genome Res*, 13, 2498-2504, doi:10.1101/gr.1239303, 2003.

641 645 Shi, Z., Allison, S. D., He, Y., Levine, P. A., Hoyt, A. M., Beem-Miller, J., Zhu, Q., Wieder, W. R., Trumbore, S., and Randerson, J. T.: The age distribution of global soil carbon inferred from radiocarbon measurements, *Nature Geoscience*, 13, 555-559, doi:10.1038/s41561-020-0596-z, 2020.

646 Silver, W. L., Neff, J., McGroddy, M., Veldkamp, E., Keller, M., and Cosme, R.: Effects of Soil Texture on Belowground Carbon and Nutrient Storage in a Lowland Amazonian Forest Ecosystem, *Ecosystems*, 3, 193-209, doi:10.1007/s100210000019, 2000.

647 650 Six, J., Callewaert, P., Lenders, S., De Gryze, S., Morris, S., Gregorich, E., Paul, E., and Paustian, K.: Measuring and understanding carbon storage in afforested soils by physical fractionation, *Soil science society of America journal*, 66, 1981-1987, 2002.

651 Song, W., Tong, X., Liu, Y., and Li, W.: Microbial Community, Newly Sequestered Soil Organic Carbon, and $\delta^{15}\text{N}$ Variations Driven by Tree Roots, *Front Microbiol*, 11, doi:10.3389/fmicb.2020.00314, 2020.

652 655 Sparks, D. L., Page, A. L., Helmke, P. A., Loeppert, R. H., Soltanpour, P. N., Tabatabai, M. A., Johnston, C. T., and Sumner, M. E.: Methods of soil analysis. Part 3 - chemical methods, *Soil Biology and Biochemistry*, 96, 74-81, doi:10.1016/j.soilbio.2016.01.016, 2016.

656 660 Stuiver, M. and Polach, H. A.: Discussion Reporting of ^{14}C Data, *Radiocarbon*, 19, 355-363, doi:10.1017/S0033822200003672, 1977.

661 Šturová, M., Bárta, J., Šantrůčková, H., and Baldrian, P.: Small-scale spatial heterogeneity of ecosystem properties, microbial community composition and microbial activities in a temperate mountain forest soil, *FEMS Microbiology Ecology*, 92, doi:10.1093/femsec/fiw185, 2016.

Taylor, M.: Determination of total phosphorus in soil using simple Kjeldahl digestion, *Communications in Soil Science and Plant Analysis*, 31, 2665-2670, 2000.

665 Telles, E. d. C. C., de Camargo, P. B., Martinelli, L. A., Trumbore, S. E., da Costa, E. S., Santos, J., Higuchi, N., and Oliveira Jr, R. C.: Influence of soil texture on carbon dynamics and storage potential in tropical forest soils of Amazonia, *Global Biogeochemical Cycles*, 17, 2003.

Torn, M. S., Trumbore, S. E., Chadwick, O. A., Vitousek, P. M., and Hendricks, D. M.: Mineral control of soil organic carbon storage and turnover, *Nature*, 389, 170-173, doi:10.1038/38260, 1997.

670 Turner, S., Mikutta, R., Meyer-Stüve, S., Guggenberger, G., Schaarschmidt, F., Lazar, C. S., Dohrmann, R., and Schippers, A.: Microbial Community Dynamics in Soil Depth Profiles Over 120,000 Years of Ecosystem Development, *Front Microbiol*, 8, doi:10.3389/fmicb.2017.00874, 2017.

Urbanová, M., Šnajdr, J., and Baldrian, P.: Composition of fungal and bacterial communities in forest litter and soil is largely determined by dominant trees, *Soil Biology and Biochemistry*, 84, 53-64, doi:10.1016/j.soilbio.2015.02.011, 2015.

675 Valentine, D. L.: Adaptations to energy stress dictate the ecology and evolution of the Archaea, *Nature Reviews Microbiology*, 5, 316-323, doi:10.1038/nrmicro1619, 2007.

Wagner, L., Stielow, B., Hoffmann, K., Petkovits, T., Papp, T., Vágvölgyi, C., De Hoog, G., Verkley, G., and Voigt, K.: A comprehensive molecular phylogeny of the Mortierellales (Mortierellomycotina) based on nuclear ribosomal DNA, *Persoonia-Molecular Phylogeny and Evolution of Fungi*, 30, 77-93, 2013.

680 Wang, C., Houlton, B. Z., Liu, D., Hou, J., Cheng, W., and Bai, E.: Stable isotopic constraints on global soil organic carbon turnover, *Biogeosciences*, 15, 987-995, doi:10.5194/bg-15-987-2018, 2018.

Wang, Q., Garrity, G. M., Tiedje, J. M., and Cole, J. R.: Naive Bayesian classifier for rapid assignment of rRNA sequences into the new bacterial taxonomy, *Applied and environmental microbiology*, 73, 5261-5267, 2007.

Will, G. and Stone, E.: Pumice soils as a medium for tree growth. 1. Moisture storage capacity, *New Zealand Journal of Forestry*, 12, 189-199, 1967.

685 Wynn, J. G., Bird, M. I., and Wong, V. N.: Rayleigh distillation and the depth profile of 13C/12C ratios of soil organic carbon from soils of disparate texture in Iron Range National Park, Far North Queensland, Australia, *Geochimica et cosmochimica acta*, 69, 1961-1973, 2005.

Xu, T., Chen, X., Hou, Y., and Zhu, B.: Changes in microbial biomass, community composition and diversity, and functioning with soil depth in two alpine ecosystems on the Tibetan plateau, *Plant and Soil*, 459, 137-153, doi:10.1007/s11104-020-04712-z, 2021.

690 Yang, Y., Li, T., Wang, Y., Cheng, H., Chang, S. X., Liang, C., and An, S.: Negative effects of multiple global change factors on soil microbial diversity, *Soil Biology and Biochemistry*, 156, 108229, doi:10.1016/j.soilbio.2021.108229, 2021.

Yost, J. L. and Hartemink, A. E.: How deep is the soil studied – an analysis of four soil science journals, *Plant and Soil*, 452, 5-18, doi:10.1007/s11104-020-04550-z, 2020.

695 Yu, G., Smith, D. K., Zhu, H., Guan, Y., and Lam, T. T.-Y.: ggtree: an r package for visualization and annotation of phylogenetic trees with their covariates and other associated data, *Methods in Ecology and Evolution*, 8, 28-36, doi:10.1111/2041-210X.12628, 2017.

Yurkov, A. M., Wehde, T., Federici, J., Schäfer, A. M., Ebinghaus, M., Lotze-Engelhard, S., Mittelbach, M., Prior, R., Richter, C., Röhl, O., and Begerow, D.: Yeast diversity and species recovery rates from beech forest soils, *Mycological Progress*, 15, 845-859, doi:10.1007/s11557-016-1206-8, 2016.

Zhelnina, K., Dias, R., de Quadros, P. D., Davis-Richardson, A., Camargo, F. A., Clark, I. M., McGrath, S. P., Hirsch, P. R., and Triplett, E. W.: Soil pH determines microbial diversity and composition in the park grass experiment, *Microbial ecology*, 69, 395-406, 2015.

700 Zhang, C., Tayyab, M., Abubakar, A. Y., Yang, Z., Pang, Z., Islam, W., Lin, Z., Li, S., Luo, J., Fan, X., Fallah, N., and Zhang, H.: Bacteria with Different Assemblages in the Soil Profile Drive the Diverse Nutrient Cycles in the Sugarcane Straw Retention Ecosystem, *Diversity*, 11, 194, 2019.